Adsorption Study of Phenol and some Phenol Derivatives on Fe_3O_4/C Nanocomposites

Roxana Istratie[1*], Cornelia Păcurariu, Robert Ianoș

[1]Politehnica University Timişoara, Faculty of Industrial Chemistry and Environmental Engineering, 6 Pîrvan Blv., RO-300223, Timişoara, Romania
e-mail: roxana.istratie@upt.ro

Abstract
Magnetite/carbon nanocomposites, prepared by a simple combustion synthesis technique, were tested for the removal of phenol and of some phenol derivatives: p-chlorophenol (p-CP), 3-aminophenol (3-AP), p-nitrophenol (p-NP), 2,6-dimethylphenol (DMP) and 2,4,6-trimethylphenol (TMP) from aqueous solutions. The effect of different parameters, including the magnetite/carbon ratio, initial concentration of pollutant and the contact time on the removal efficiency was investigated. The adsorption kinetics was described by the pseudo-second-order model and the equilibrium data were well fitted with the Langmuir isotherm in case of phenol, the Sips isotherm in case of 3-aminophenol and the Redlich-Peterson isotherm in case of p-nitrophenol. The good adsorption capacity and easy separation using a magnet, recommend the magnetite/carbon nanocomposites as promising candidates for the removal of phenol and its derivatives from polluted water.

***Keywords**: iron oxides, nanocomposites, adsorption, phenol*

Introduction
Water contamination with aromatic compounds is a usual problem of our days. Among the aromatic compounds which are in wastewater from different industries like: petroleum, paper, paint, resins, pharmaceutics, phenols and their derivatives are an important category. They were classified like priority pollutants by US Environmental Protection Agency (EPA) and UE because of their toxicity, causing specific taste and odor in drinking water with possible negative effects for biological processes [1]. Repeated exposure to phenols and to their derivatives could cause negative effects to nervous system, digestive system, eyes, heart, lungs, liver, kidney, skin and can cause genetic damages [2].
Throughout time there were developed many techniques for the removal of phenols from wastewater such as: oxidation [3], membrane filtration [4], electrochemical oxidation [5], photocatalytic degradation [6], adsorption [7, 8], ion exchange [9], solvent extraction [10] etc.
Among this methods, adsorption is considered by many authors to be a superior technique because of its efficiency, low implementation cost, large availability and simplicity of design [11-16]. However, usual adsorbents have some limitations because of their difficult separation from the solution [17, 18]. Due to these reasons, magnetic nanoparticles have drawn the researchers' attention because of their high adsorption capacity and their effectiveness regarding the separation [19-25].
The aim of this work was to investigate the efficiency of some magnetite/carbon nanocomposites as adsorbents for the removal of phenol and some phenol derivatives: p-chlorophenol (p-CP), 3-aminophenol (3-AP), p-nitrophenol (p-NP), 2,6-dimethylphenol (DMP) and 2,4,6-trimethylphenol (TMP) from aqueous solutions. The effect of different parameters, including the magnetite/carbon ratio, initial concentration of pollutant and the contact time on the removal efficiency was investigated. The kinetics and adsorption isotherm were also evaluated.

Experimental

2.1.Powder preparation

The magnetite/carbon nanocomposites were prepared by the combustion synthesis method as described in our earlier work [26]. The solution resulted from the dissolution of necessary amount of Fe(NO3)3·9H2O and tartaric acid (C4H6O6) in distilled water was mixed with different quantities of carbon in a bottom flask. The flask was placed inside a heating mantle at 400 °C. As the temperature increased, a smoldering combustion reaction occurred between iron nitrate and tartaric acid. The gases evolving from the combustion process were bubbled in a beaker filled with distilled water, to prevent air getting inside the flask.
After 30 minutes a black powder was obtained. The product was washed with distilled water and dried at 70ºC for 5 h.

2.2.Characterization methods

The nanocomposites characterization by means of phase composition (XRD), FTIR spectroscopy, thermal analysis (TG/DTA), magnetic properties and morphology was reported in our previous work [26].

2.3.Adsorption experiments

The experiments of adsorption of phenol, p-chlorophenol (p-CP), 3-aminophenol (3-AP), p-nitrophenol (p-NP), 2,6-dimethylphenol (DMP) and 2,4,6-trimethylphenol (TMP) from aqueous solutions were performed at 25ºC, in a thermostated shaker with a shaking speed of 200 rpm, using 1 g L-1 adsorbent and different initial concentration of pollutants (50 – 300 mgL-1). The adsorbent was separated from the aqueous solution using a magnet. The pollutants concentration was measured using a UV – Vis spectrophotometer model UVmini – 1240 SHIMADZU. The absorbance values were measured at 270 nm for phenol, 280 nm for p-CP and 3-AP, 317 nm for p-NP, 217 nm for DMP and 218 nm for TMP.
The amount of pollutant adsorbed, qt (mg g-1), was calculated according to Eq. (1):

$$q_t = \frac{(C_0 - C_t)\cdot V}{W} \qquad (1)$$

where Co and Ct are the concentration of pollutants, initially and, respectively, at any time, t, V is the volume of solution (L) and W is the mass of adsorbent (g).
The removal efficiency R (%) was calculated by Eq (2):

$$R = \frac{C_0 - C_e}{C_0}\cdot 100 \qquad (2)$$

where C_o and C_e (mg L^{-1}) are the initial and the equilibrium concentration of pollutants.

Results and discussion

3.1.Characterization of the samples

Some characteristics of the samples are presented in Table 1.

Table 1. Characteristics of the prepared samples

Sample symbol	Fe_3O_4/carbon mass ratio	Specific surface aria $S_{BET}(m^2g^{-1})$	Micropore aria (m^2 g^{-1})	Micropore volume (cm^3 g^{-1})	Particle diameter D_{BET} (nm)	Phase composition XRD
M1-C3	1/3	622.4	390.9	0.178	1.85	Fe_3O_4
M1-C10	1/10	813.5	505.6	0.234	1.42	Fe_3O_4

3.2. Adsorption studies

Effect of pollutant nature

The studies were effectuated in the following conditions: mass of adsorbent 1 g L-1, initial concentration of the pollutant C0, 100 mg L-1, temperature 25ºC, contact time 6 h, shaking speed 200 rpm. The influence of pollutant nature on the adsorption capacity of the adsorbents is presented in Table 2.

Table 2. Effect of pollutant nature on the adsorption capacity of adsorbents

Adsorbent	Adsorbed	Solubility at 25°C [g L^{-1}]	pK_a	R[%]
M1-C3	Phenol	83	9.95	65.2
	p-CP	24	9.42	91.8
	3-AP	35	4.30	75.5
	p-NP	16	7.15	96.9
	DMP	10	10.59	90.3
	TMP	1.2	10.88	95.7
M1-C10	Phenol	83	9.95	73.9
	p-CP	24	9.42	95.0
	3-AP	35	4.30	89.1
	p-NP	16	7.15	98.2
	DMP	10	10.59	97.8
	TMP	1.2	10.88	98.4

As can be observed, both adsorbents present higher removal efficiency in the case of phenol derivatives as compared to phenol. This behavior was correlated with the solubility and pKa values of pollutants, factors that have a significant influence on the adsorption process.

For practically equal pKa values, both adsorbents present higher removal efficiency for the less soluble pollutant (phenol compared with p-CP, respectively DMP compared with TMP). The solubility of p-CP is much lower as compared with phenol, while its removal efficiency is much higher. TMP is much less soluble as compared with DMP and its removal efficiency is higher. In case of pollutants with similar solubility, higher removal efficiency can be observed for the pollutant with the smaller pKa value.

Effect of magnetite/carbon ratio

The effect of magnetite/carbon ratio on the removal efficiency of pollutants is presented in

Figure 1.

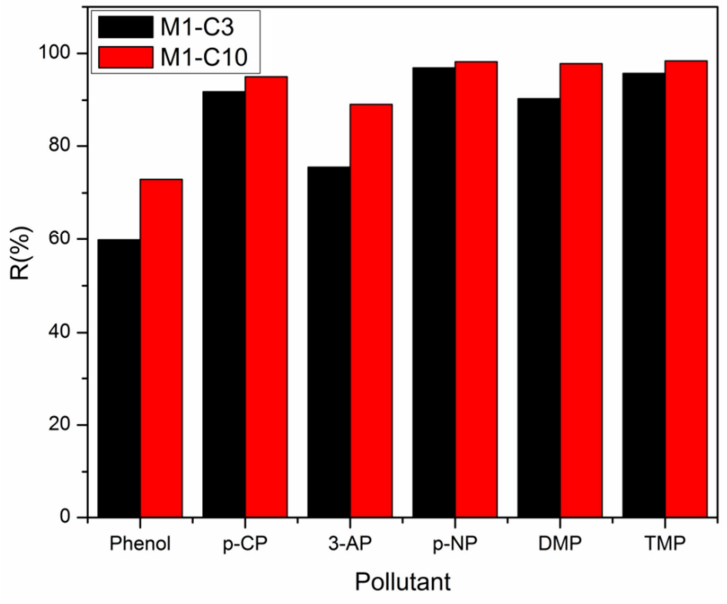

Figure 1. The effect of emagnetite/carbon ratio on the removal efficiency of pollutants.

From Table 2 and Fig. 1 it can be observed that the adsorbent M1-C10, with higher carbon content (1/10) presents higher removal efficiency of phenol, respectively of phenol derivatives compared to M1-C3 adsorbent that has a lower content of carbon (1/3). This behavior is correlated with the specific surface area that is higher for M1-C10 adsorbent (813.5 m2g-1) compared to M1-C3 (622.4 m2 g-1). The significantly increase of carbon content in case of M1-C10 adsorbent does not lead to a spectacular increase of the removal efficiency; therefore is not justified to use an adsorbent with high content of carbon due to higher costs and a lower magnetization which require the use of stronger magnets for phase separation. For these reasons, the following adsorption studies were performed using only M1-C3 as adsorbent and phenol, 3-AP and p-NP as pollutants.

Effect of initial pollutant concentration

Fig. 2 shows the effect of initial pollutant concentration on the adsorption process.

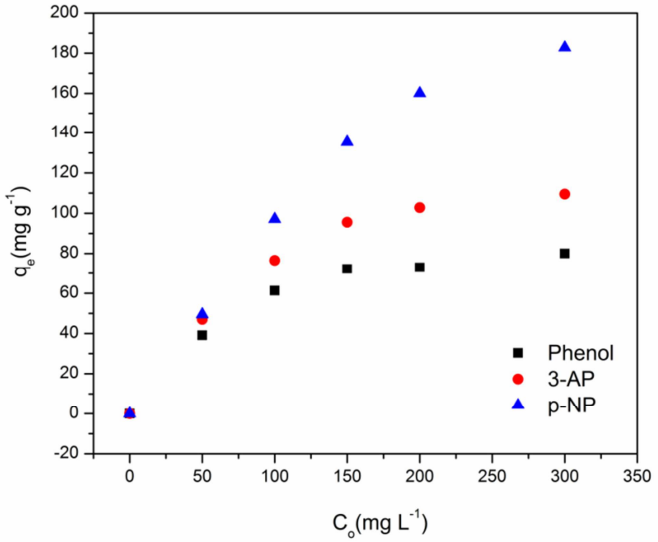

Figure 2. Effect of initial concentration on phenol, 3-AP and p-NP adsorption using M1-C3 adsorbent

In case of phenol, the adsorbed amount at equilibrium continuously increases for initial

concentration between 0-150 mg L-1 and after that, it remains constant; this behavior can be explained by the saturation of the adsorbent surface with phenol.
In case of p-nitrophenol, it can be observed that the adsorbed amount at equilibrium increases over the entire concentrations range, confirming that the adsorbent M1-C3 shows the highest adsorption capacity for p-nitrophenol, in accordance with the previous results (Fig.1).

Effect of contact time
Figure 3 shows the effect of contact time on phenol, p-nitrophenol and 3-aminophenol adsorption onto M1-C3 adsorbent. It can be observed the fast increase of the amount of adsorbed pollutants in the first 20 minutes which can be attributed to the large number of vacant surface sites available at the initial stage of adsorption; then, the adsorption process becomes slower, as the system approaches equilibrium. It can be noticed that the equilibrium was reached faster in case of p-NP (about 30 min.) as compared with 3-AP and phenol (about 240 min).

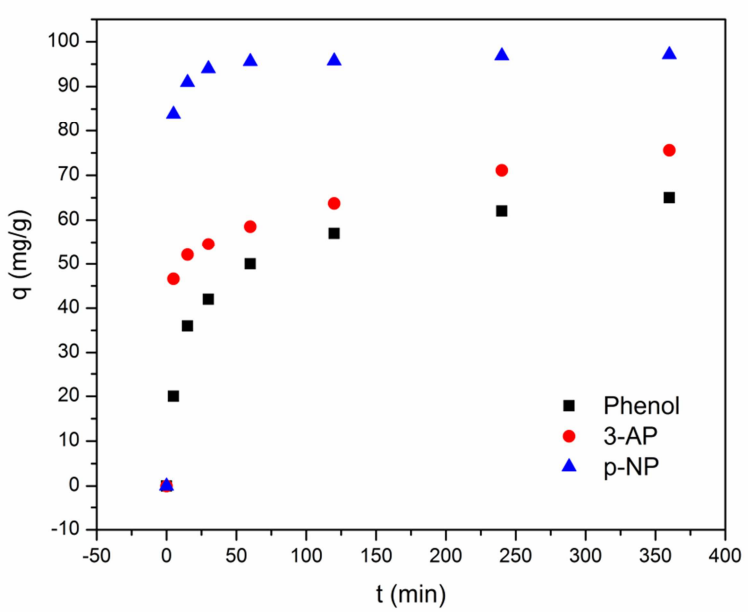

Figure 3. Effect of contact time on phenol, 3-AP and p-NP adsorption using M1-C3 adsorbent

Adsorption kinetics
The adsorption kinetics of the 3 pollutants onto M1-C3 adsorbent was investigated by fitting the experimental data with the linear form of the pseudo-second-order (Eq. 3).

$$\frac{t}{q_t} = \frac{1}{k_2 q_e^2} + \frac{t}{q_e} \quad (3)$$

were k2 is the pseudo-second-order rate constant (g mg-1 min-1); qe and qt are the amount of pollutant adsorbed at equilibrium and at time t per unit mass of adsorbent, respectively (mg g-1).
The results are shown in Fig. 4 and Table 3.

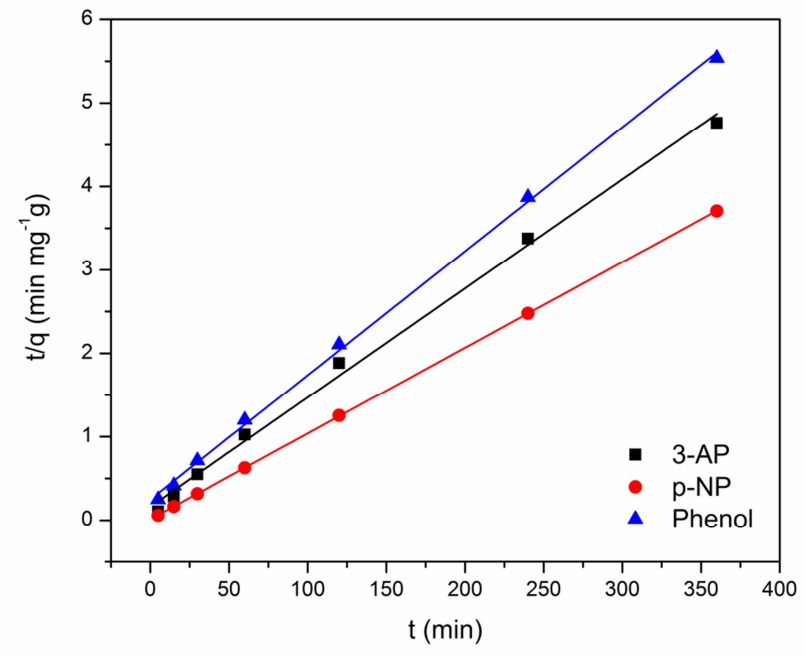

Figure 4. Plots of t/q=f(t) dependencies for the adsorption of phenol, 3-AP and p-NP onto M1-C3 adsorbent

Table 3. Kinetics parameters and corelation coeficients for the pseudo-second-order model

Pollutant	Initial concentration C_o (mg L^{-1})	$k_2 \cdot 10^3$ (g mg^{-1} min^{-1})	q_e(mg g^{-1})		R^2
			Experimental	Calculated	
Phenol	100	0.88	65.2	67.3	0.99878
3-AP	100	1.05	75.6	76.4	0.99575
p-NP	100	8.79	97.1	97.4	0.99999

The correlation coefficients close to unity and experimental values for qe very close to the calculated ones indicate that the adsorption kinetics of the 3 pollutants onto M1-C3 adsorbent is described by the pseudo-second-order model.
It can be noticed that, the rate constant in case of p-NP adsorption is about 10 times higher than that of phenol adsorption and about 8 times higher than that of 3-AP adsorption. These results are in full agreement with the shorter time to reach equilibrium in case of p-NP as compared with phenol and 3-AP.

Adsorption isotherms
The experimental equilibrium data for the adsorption of the 3 pollutants onto M1-C3 adsorbent were fitted to the Langmuir, Freundlich, Redlich-Peterson and Sips isotherms by plotting qe versus Ce (Figs. 5-7).
The isotherms parameters, calculated by non-linear regression analysis and the correlation coefficients are listed in Table 4.

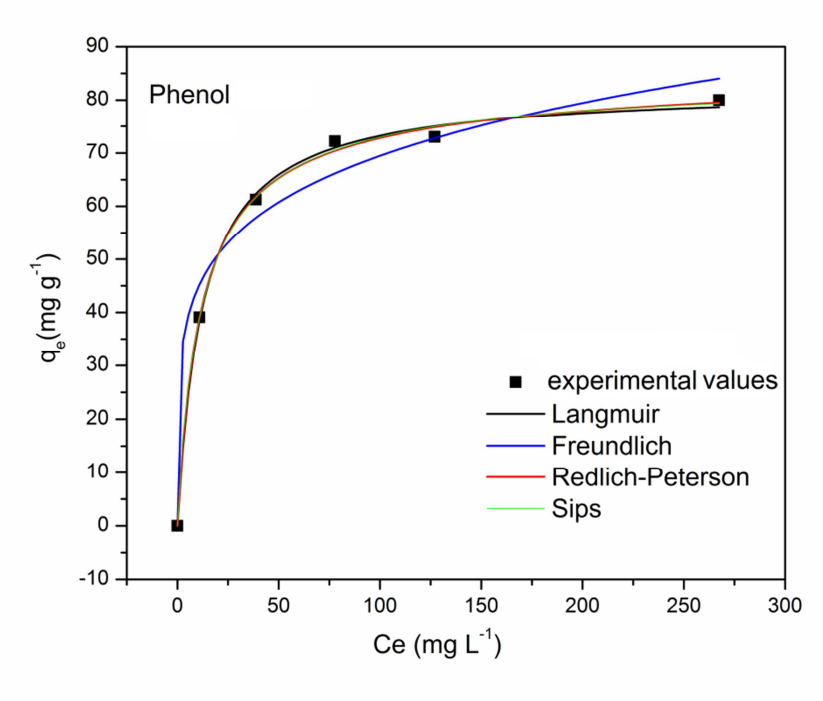

Figure 5. Isotherm plots for phenol adsorption onto M1-C3 sorbent.

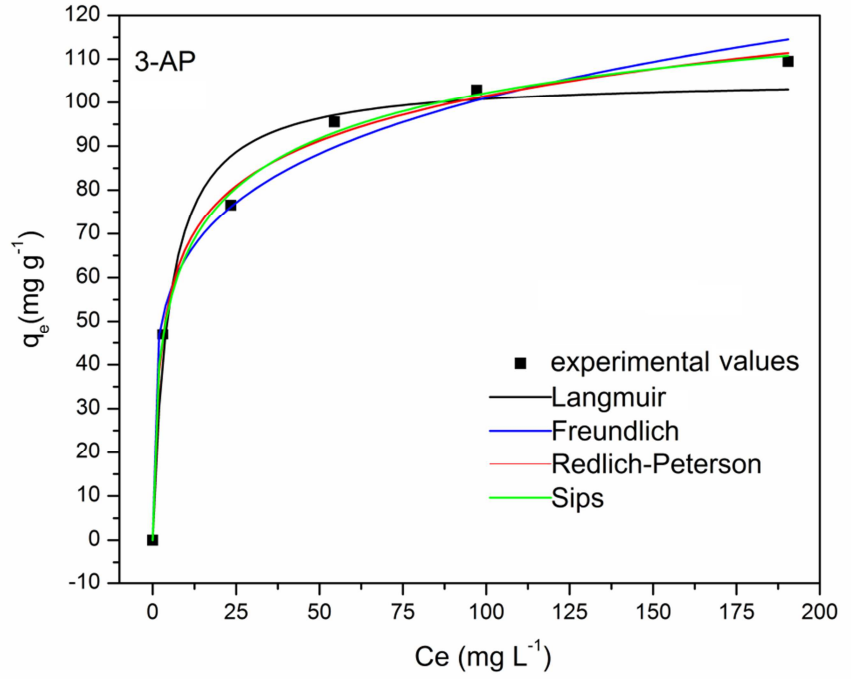

Figure 6. Isotherm plots for 3-AP adsorption onto M1-C3 sorbent

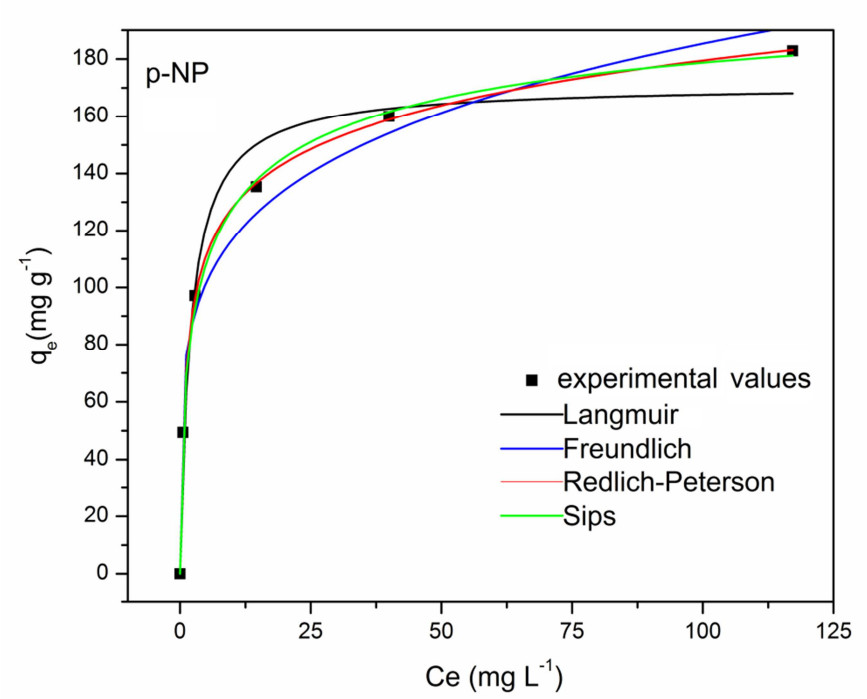

Figure 7. Isotherm plots for p-NP adsorption onto M1-C3 sorbent

Table 4. The isotherms parameters and correlation coefficients for the adsorption of phenol, 3-AP and p-NP onto M1-C3 adsorbent

		Phenol	3-AP	p-NP
Langmuir	K_L (L mg^{-1})	0.08	0.21	0.49
	q_m(mg g^{-1})	82.34	105.62	170.99
	R^2	**0.99762**	0.96998	0.96831
Freundlich	K_F (((mg$^{1-(1/n)}$L$^{1/n}$)g^{-1}))	28.50	41.20	73.58
	n	5.17	5.13	4.98
	R^2	0.9718	0.98823	0.97478
Redlich-Peterson	K_{RP} (L g^{-1})	7.32	53.13	183.06
	α_{RP} ((L mg^{-1})$^{\beta}$)	0.10	0.94	1.75
	β	0.97	0.87	0.88
	R^2	0.9975	0.99457	**0.99978**
Sips	K_S (L mg^{-1})	0.10	0.28	0.43
	q_{mS}(mg g^{-1})	84.53	146.75	215.99
	n	0.90	0.28	0.52
	R^2	0.99737	**0.99668**	0.99732

As shown in Fig. 5 and Table 4, in case of phenol, the best fit of the experimental data was obtained by the Langmuir isotherm (R2>0.99762). The maximum adsorption capacity of M1-C3 adsorbent in case of phenol is qe=82.34 mg g-1. The adsorption of 3-aminophenol onto M1-C3 adsorbent is described by the Sips isotherm and the adsorption of p-nitrophenol is described by the Redlich-Peterson isotherm. Comparing the maximum adsorption capacity obtained with the Langmuir isotherm, respectively with the Sips isotherm for the 3 pollutants, there was confirmed the increase of the adsorption capacity of M1-C3 adsorbent in the order: phenol<3-aminophenol<p-nitrophenol.

The values of "n" parameter from Freundlich isotherm, between 4.98 and 5.17, indicate that the adsorption of the 3 pollutants on M1-C3 adsorbent is favored. In the case of phenol adsorption on carbon, the literature data indicate "n" values between 2.793 and 6.821 [27].

Conclusion

The adsorption studies have demonstrated the efficiency of using magnetite/carbon nanocomposites for the removal of phenol and its derivatives from aqueous solutions. It was demonstrated that both studied adsorbents, M1-C3 and M1C10, with different carbon content, show a higher adsorption capacity for pollutants less soluble and with lower pKa value.
The increase of carbon content from 1:3 for M1-C3 to 1:10 in case of M1-C10 adsorbent has led to a moderate increase of removal efficiency for both, phenol and its derivatives. This behavior can be explained by the increase of the specific surface area of M1-C10 adsorbent.
The increase of the initial concentration of pollutant determines the increase of adsorbed quantity at equilibrium; the least in case of phenol and the most in case of p-nitrophenol.
The adsorption process is very fast; the contact time to reach equilibrium is about 30 min for p-nitrophenol and approximately 240 min for phenol and 3-aminophenol, in the case of M1-C3 adsorbent.
The kinetics of adsorption process of phenol, 3-aminophenol and p-nitrophenol onto M1-C3 adsorbent is described by the pseudo-second-order model. The rate of adsorption process increases in the order: phenol<3-aminophenol<p-nitrophenol.
The adsorption process of phenol is described by the Langmuir isotherm, 3-aminophenol by Sips isotherm and p-nitrophenol by Redlich-Peterson isotherm. Comparing the maximum adsorption capacity of obtained with the Langmuir isotherm respectively with the Sips isotherm for the 3 pollutants, it was confirmed the increase of the adsorption capacity of M1-C3 adsorbent in the order: phenol<3-aminophenol<p-nitrophenol.
In conclusion, the studied magnetite/carbon nanocomposites show both, high adsorption capacity due to the carbon content and easy phase separation using a magnet.
The unique combination between high adsorption capacity, excellent separation capacity and short time to reach equilibrium, that implies low operational costs for the industrial adsorption systems, indicate that the investigated magnetite/carbon nancomposites are excellent adsorbent materials with great potential for wastewater treatment at industrial scale.

Acknowledgements

This work was partially supported by the strategic grant POSDRU/159/1.5/S/137070 (2014) of the Ministry of National Education, Romania, co-financed by the European Social Fund – Investing in People, within the Sectoral Operational Programme Human Resources Development 2007-2013.

References

[1] G. Yanga, L. Tang, Y. Caia, J. Tanga, B. Y. Pangc, Y. Zhoua, Y. Liua, J. Wanga, S. Zhanga, W. Xionga, Chem. Eng. J. 259 (2015) 854 – 864.
[2] J. Fu, Z. Chen, M. Wang, S. Liu, J. Zhang, R. Han, Q. Xu, Chem. Eng. J. 259 (2015) 53 – 61.
[3] J. Wu, J. Rudy, J. Spark, Adv. Environ. Res. 4 (2000) 339 – 346.
[4] D. P. Zagklis, A. I. Vavourakia, M. E. Kornarosa, C. A. Paraskeva, J. Hazard. Mater 285 (2015) 69 – 76.
[5] F. Duana, Y. Li, H. Cao, Y. Wanga, J. C. Crittendenc, Y. Zhang, Chemosphere 125 (2015) 205–211.
[6] Z. F. Guo, R. X. Ma, G. J. Li, Chem. Eng. J. 119 (2006) 55 – 59.
[7] V. V. Panic, Z. P. Madzarevic, T. Volkov-Husovic, S.J. Velickovic, Chem. Eng. J. 217 (2013) 192 – 204.
[8] L. Damjanovic, V. Rakic, V. Rac, D.S.A. Auroux, J. Hazard. Mater. 184 (2010) 477 – 484.
[9] K. Abburi, J. Hazard. Mater. 105 (2003) 143 – 156.
[10] A. Gomes, L. Fernandes, R. Simoes, Chem. Eng. J. 189 – 190 (2012) 175 -181.
[11] J. Han, Z. Du, W. Zou, H. Li, C. Zhang, Chem. Eng. J. 262 (2015) 571 – 578.
[12] A. Turki, C. Guillardb, F. Dappozzeb, Z. Ksibia, G. Berhaultb, H. Kochkara, Appl. Catal. B-Environ. 163 (2015) 404 – 414.
[13] Ihsanullaha, H. A. Asmalya, T. A. Salehb, T. Laouie, V. K. Guptac, M.A. Atieh, J. Mol. Liq. 206 (2015) 176 – 182.
[14] B. Tanhaei, A. Ayatia, M. Lahtinenb, M. Sillanpää, Chem. Eng. J. 259 (2015) 1 – 10.
[15] L. Zeng, M. Xie, Q. Zhang, Y. Kang, X. Guo, H. Xiao, Y. Peng, J. Luo, Carbohyd. Polym. 123 (2015) 89 – 98.
[16] K.L. Ai, Y.L. Liu, C.P. Ruan, L.H. Lu, G.Q. Lu, Adv. Mat. J. 25 (2013) 998 – 1003.
[17] B. Noroozi, G.A. Sorial, H. Bahrami, M. Arami, J. Hazard. Mat. 139 (2007) 167 – 174.
[18] Q. Q. Liu, L. Wang, A. G. Xiao, J.G. Gao, W. B. Ding, H.J. Yu, J. Huo, J. Hazard. Mat. 181 (2010) 586 – 592.
[19] G. Z. Kyzas, K. A. Matisa, J. Mol. Liq. 203 (2015) 159 – 168.
[20] S. Lia, Y. Gonga, Y. Yanga, C. Hea, L. Hua, L. Zhua, L. Suna, D. Shu, Chem. Eng. J. 260 (2015) 231 – 239.
[21] L.H. Reddy, J.L. Arias, J. Nicolas, P. Couvreur, Chem. Rev. 112 (2012) 5818 – 5878.
[22] I. Ali, Chem. Rev. 112 (2012) 5073 – 5091.
[23] S.C.N. Tang, I.M.C. Lo, Water Res. 47 (2013) 2613 – 2632.
[24] A. H. Lu, E. I. Salabas, F. Schuth, Angew. Chem. Int. Edit. 46 (2007) 1222 – 1244.
[25] R.D. Ambashta, M. Sillanpaa, J. Hazard. Mater. 180 (2010) 38 – 49.
[26] R. Ianoș, C. Păcurariu, G. Mihoc, Ceram. Int. 40(8) (2014) 13649 – 13657.
[27] O. Hamdaoui, E. Naffrechoux, J. Hazard. Mater. 147 (2007) 381–394.